Subgrid Modeling of Unsteady Two-Phase Turbulent Flows*

Suresh Menon[†] **and Sreekanth Pannala**[‡]
School of Aerospace Engineering
Georgia Institute of Technology
Atlanta, GA 30332-0150

Abstract

A subgrid scalar mixing and combustion model originally developed for gas phase combustion has been extended in this study to include the liquid phase. This approach includes a more fundamental treatment of the effects of the final stages of droplet vaporization, molecular diffusion, chemical reactions and small scale turbulent stirring than other LES closure techniques. As a result, Reynolds, Schmidt and Damkohler number effects are explicitly included. This model has been implemented within an Eulerian-Lagrangian two phase large-eddy simulation (LES) formulation. In this approach, the liquid droplets are tracked using the Lagrangian approach up to a pre-specified cut-off size. The evaporation and mixing of the droplets smaller than the cutoff size is modeled within the subgrid using an Eulerian two-phase model that is an extension of the earlier gas-phase subgrid model. The issues related to the implementation of this subgrid model within the LES are discussed in this paper along with some preliminary results that demonstrate its capabilities.

1. Introduction

Combustion efficiency, reduced emissions and stable combustion in the lean limit are some of the desirable features in the next generation gas turbine engines. To achieve these capabilities, current research is focussing on improving the liquid fuel atomization process and to increase fuel-air mixing downstream of the fuel injector. To characterize the mixing process, the details at the small scales are needed. Experimental non-intrusive techniques have some inherent limitations in terms of resolving these small-scale details. For example, the near field of a liquid fuel injector has never been properly investigated due to difficulties in carrying out measurements in dense droplet regimes. Structure of complex three-dimensional, swirling fuel-air mixing layers is also very difficult to resolve using current experimental methods. There are also some fundamental problems in carrying out numerical studies of fuel atomization and fuel-air mixing. Since both these processes are highly unsteady conventional steady state methods cannot be used to elucidate the finer details. On the other hand, although unsteady mixing process can be studied quite accurately using direct numerical simulation (DNS) (e.g., Poinsot, 1996), application of DNS is limited to low to moderate Reynolds numbers (Re) due to resolution requirements. This restriction limits the extension of conclusions drawn from DNS results to high Reynolds number complex flows typical in a gas turbine combustors. An alternative approach called large-eddy simulation (LES) has the potential for application to high Re flows. However, the application of LES to reacting flows requires demonstrable ability to capture the effects of turbulent small-scale mixing and chemical reactions.

In LES, the scales larger than the grid size are computed using a time- and space-accurate scheme, while the unresolved smaller scales, which are mostly isotropic, are modeled using an eddy viscosity based subgrid model. Closure of the momentum and energy transport equations can be achieved using this method since the small scales primarily provide a dissipative mechanism for the energy transferred from the large scales. However, for combustion to occur, the species must first undergo mixing and come into molecular contact. These processes occur at the small scales which are not resolved in conventional LES approach. As a result, conventional subgrid eddy diffusivity models cannot be used to model these features.

To address these issues, recently (Menon et al., 1993a; Menon and Calhoon, 1996; Calhoon and Menon, 1996, 1997), a subgrid combustion model was developed and implemented within the LES formulation. This model separately and simultaneously treats the physical processes of molecular diffusion and small scale turbulent convective stirring. This is in contrast to probability density function closure which phenomenologically treats these two processes by a single model, thereby removing experimentally observed Schmidt number variation of the flow. The capabilities of this model have been demonstrated in the above noted studies by carrying out quantitative comparison with high-Re experimental data obtained in

†. Professor, Senior Member, AIAA
‡. GRA, Student Member, AIAA

reacting shear layers. Application of this method to premixed combustion has also been recently demonstrated (Menon et al., 1993b; Smith, Menon and Chakravarthy, 1996; Chakravarthy and Menon, 1997. Results show that this method can capture thin, high-Re turbulent flames without any numerical dissipation. The predicted turbulent flame speed was also shown to be in reasonable agreement with high-Re data.

The above methodology was originally developed to study gas phase combustion. To apply this method to investigate liquid fuel droplet vaporization and fuel-air mixing requires some additional modifications. This paper discusses the issues related to this development and presents some preliminary results for two-phase flows in both non-reacting and reacting mixing layers.

2. Formulation of the Two-Phase LES Model

Both Eulerian and Lagrangian formulations have been used to simulate two-phase flows in the past (e.g., Mostafa and Mongia, 1983). Both methods have their own merits and demerits; however, most state-of-the-art codes employ the Lagrangian form to capture the droplet dynamics, while the gas phase is still computed in the Eulerian form (e.g., Oefelein and Yang, 1996). In this formulation, the droplets are tracked explicitly using Lagrangian equations of motion, and, heat and mass transfer are computed for each droplet. Due to resource constraints (computer time and memory), only a limited range of droplet sizes are computed. Droplets below an *ad hoc* cut-off size are assumed to vaporize instantaneously and to become fully mixed in the gas phase. This is a critical assumption and flawed, since (as noted above), even in pure gas phase flows it has been determined that the small-scale mixing process is very important for quantitative predictions. The final stages of droplet vaporization and the subsequent mixing needs to be properly resolved for accurate prediction of the combustion process. Here, the gas-phase subgrid combustion methodology has been extended to allow proper simulation of the final stages of droplet evaporation and turbulent mixing.

The two-phase subgrid process is implemented within the framework of the Eulerian-Lagrangian LES approach. Thus, droplets larger than the cut-off size are tracked as in the usual Lagrangian approach. However, once the droplets are smaller than the cutoff, a two-phase subgrid Eulerian model is employed to include the effects of the small droplets within the LES cells. In the following, the details of the Lagrangian LES model and the new subgrid two-phase combustion model are briefly described.

2.1 Gas Phase LES Equations

Our present approach employs the incompressible Navier Stokes equations in the zero Mach number limit since most of the characteristic problems currently under study are predominantly isobaric and can be solved efficiently using this approach. The extension to fully compressible flows (with acoustic wave motion) will be considered at a future date. No fundamental problems in extending the subgrid two-phase model to compressible flows are expected. Zero-Mach number approach involves using a series expansion in terms of Mach number to remove the acoustic component from the compressible Navier-Stokes equations and is a well established method (McMurtry et al., 1989; Chakravarthy and Menon, 1997). A key feature of this expansion is that the pressure field is split into two parts: a kinematic pressure (p) related to the velocity field and a thermodynamic pressure $(\hat{p})$ that must be specified.

To obtain the LES equations, the low-Mach number equations are filtered using a specified filter function to remove the contribution of the scales smaller than the grid size. The filter function can be of any type, however, for the present finite-difference approach a top-hat function is employed. The resulting LES mass, momentum, energy and species equations (all LES terms are identified with a bar on top) can be written as:

$$\frac{\partial \rho}{\partial t} + \frac{\partial \rho \bar{u}_i}{\partial x_i} = \dot{\rho}_s \tag{1}$$

$$\frac{\partial \bar{u}_i}{\partial t} + \bar{u}_j \frac{\partial \bar{u}_i}{\partial x_j} = \frac{\partial \bar{p}}{\partial x_i} + \nu \frac{\partial^2 \bar{u}_i}{\partial x_k \delta x_k} + \frac{\partial \tau_{ij}}{\partial x_j} + \frac{\dot{F}_s}{\rho} \tag{2}$$

$$\frac{\partial \bar{u}_i}{\partial x_i} = \frac{1}{\hat{p}} \left[\lambda \frac{\partial^2 T}{\partial x_k \partial x_k} - \frac{\partial \hat{p}}{\partial t} + \dot{Q}_s \right] \tag{3}$$

$$\frac{\partial \rho \overline{Y_\alpha}}{\partial t} + \frac{\partial \rho \overline{Y_\alpha} u_j}{\partial x_j} = D \frac{\partial^2 \overline{Y_\alpha}}{\partial x_k \partial x_k} + \frac{\partial S_{\alpha j}}{\partial x_j} + \overline{\dot{\omega}_\alpha} + S_{s,\alpha} \tag{4}$$

The above system of equations are supplemented by the equation of state for the thermodynamic pressure $\hat{p} = \rho RT$ which can be used to obtain the temperature T. Here, $\rho, \bar{u}_i, \overline{Y_\alpha}$ and $\bar{p}$ are, respectively, the density, i-th velocity component, α-th species mass fraction and the kinematic pressure. Also, ν, λ, D and

R are, respectively, the kinematic viscosity, the thermal conductivity, the mass diffusion (assumed constant and same for all species here, but can be generalized) and the gas constant. In Eq. (4), $\dot{\omega}_\alpha$ is the LES filtered species production/destruction term which is typically a highly non-linear term and very difficult to model. Also, in the above equations, source terms $\dot{\rho}_s, \dot{F}_s, \dot{Q}_s$, and S_s represent the volume-averaged rate of exchange of mass, momentum, energy and species between the gas-phase and the liquid phase. These terms are computed, as detailed elsewhere (Oefelein and Yang, 1996; Faeth, 1983) and, therefore, omitted here for brevity. Furthermore, note that eq. (3) is the equivalent energy equation in the zero-Mach number limit. In the absence of heat release and no phase change, this equation and eq. (1) will be identical.

In the above equations, the subgrid stress tensor $\tau_{ij} = -(\overline{u_i u_j} - \bar{u}_i \bar{u}_j)$ and the species-velocity correlations $S_{\alpha j} = -(\overline{Y_\alpha u_j} - \overline{Y_\alpha}\,\bar{u}_j)$ requires modeling. In the present LES approach, the stress term τ_{ij} is modeled using the usual eddy viscosity approach as $\tau_{ij} = 2\nu_t S_{ij}$ where ν_t is the eddy viscosity and S_{ij} is the resolved rate-of-strain tensor. The subgrid eddy viscosity is obtained in terms of the grid scale $\bar{\Delta}$ and the subgrid kinetic energy, $k^{sgs} = (\overline{u_i u_i} - \bar{u}_i \bar{u}_i)$ as: $\nu_t = C_\nu k^{sgs0.5} \bar{\Delta}$. Here, k^{sgs} is obtained by solving a transport equation. More details are given elsewhere (Kim and Menon, 1995, 1996). The coefficient C_ν in the eddy viscosity model and the coefficients appearing in the k^{sgs} equation can be obtained using the dynamic procedure as described elsewhere (Kim and Menon, 1995; Menon and Kim, 1996).

It is worth noting here (and further discussed below), that the source terms $\dot{\rho}_s$, $\dot{Q}_s$ and S_s due to mass and energy transfer from the liquid to the gas phase is modeled within the subgrid domain. Furthermore, the species transport equation (4) is not solved along with the other LES equations, since, it too is modeled using the subgrid combustion approach. Thus, closure of $S_{\alpha j}$ is not needed. More details regarding the solution of the gas phase scalar equations is given elsewhere (Calhoon and Menon, 1996, 1997).

2.2 Liquid-phase LES equations

A Stochastic Separated Flow (SSF) formulation (Faeth, 1983; Oefelein and Yang, 1996) is used to track the droplets using Lagrangian equations of motion. The general equations of spherical droplets reduce to the following form when the terms arising due to static pressure gradient, virtual-mass, Besset force and external body-forces are neglected. The position and the velocity of the droplets are given by

$$\frac{dx_{p,i}}{dt} = u_i \tag{5}$$

$$\frac{du_{p,i}}{dt} = \frac{3}{4} C_D Re_p \frac{\mu}{\rho_p d_p^2}(u_i - u_{p,i}) \tag{6}$$

where the droplet properties are denoted by subscript p, d_p is the droplet diameter and u_i is the instantaneous gas phase velocities computed at the droplet location. This gas phase velocity field is obtained using both the filtered LES velocity field $\bar{u}_i$ and the subgrid kinetic energy k^{sgs} (as in the eddy interaction model). The droplet Reynolds number is computed using: $Re_p = \frac{d_p}{\nu}[(u_i - u_{p,i})(u_i - u_{p,i})]^{1/2}$ and the drag coefficient is modeled by (Faeth, 1983):

$$C_D = \begin{cases} \dfrac{24}{Re_p}\left(1 + \dfrac{1}{6} Re_p\right) & Re_p \le 10^3 \\ 0.424 & Re_p > 10^3 \end{cases} \tag{7}$$

The conservation of the mass of the droplets results is given by: $dm_p/dt = -\dot{m}_p$ where the mass transfer rate for a droplet in a convective flow field is given as:

$$\frac{\dot{m}_p}{\dot{m}_{Re_p = 0}} = 1 + \frac{0.278 Re_p^{1/2} Sc^{1/3}}{[1 + 1.232/Re_p Sc^{2/3}]^{1/2}} \tag{8}$$

Here, Sc is the Schmidt number and the subscript $Re_p = 0$ indicates quiescent atmosphere when there is no velocity difference between the gas and the liquid phase. The mass transfer under this condition is given as $\dot{m}_{Re_p = 0} = 2\pi \rho_s D_{sm} d_p \ln(1 + B_M)$. Here, ρ_s and D_{sm} are, respectively the gas mixture density and the mixture diffusion coefficient at the droplet surface and B_M is the Spalding number which is given as $B_M = (Y_{s,F} - Y_{\infty,F})/(1 - Y_{s,F})$. Here, $Y_{s,F}$ is the fuel mass fraction at the surface of the droplet and computed using the procedure described in Chen and Shuen (1993) while $Y_{\infty,F}$ is the fuel mass fraction in the ambient gas.

The heat transfer rate of the droplet (assuming uniform temperature in the droplet) is given by the following relation (Faeth, 1983):

$$m_p C_{p,p} \frac{dT_p}{dt} = h_p \pi d_p^2 (T - T_p) - \dot{m}_p \Delta h_v \qquad (9)$$

The heat transfer coefficient for a droplet in a convective flow field with mass transfer is modeled as

$$\frac{h_p}{h_{Re_p=0}} = 1 + \frac{0.278 Re_p^{1/2} Pr^{1/3}}{[1 + 1.232/Re_p Pr^{2/3}]^{1/2}} \qquad (10)$$

Here, Pr is the gas phase Prandtl number and the heat transfer coefficient for quiescent medium is given as $h_{Re_p=0} = \lambda Nu_{Re_p=0}/d_p$ where the Nusselt number is obtained from:

$$Nu_{Re_p=0} = \frac{2\ln(1 + B_M)^{Le^{-1}}}{(1 + B_M)^{Le^{-1}} - 1} \qquad (11)$$

$Nu_{Re_p=0}$ approaches a value of 2 in the case of zero mass transfer and Le is the Lewis number. Only droplets above a cut-off diameter are solved using the above equations, while the droplets below the cut-off diameter are modeled using Eulerian formulation within the subgrid.

In summary, the present LES approach for two-phase flows involves the solution of the gas phase LES equations (1)-(3) using a conventional high-accuracy finite-difference Eulerian scheme. Closure for the subgrid stresses is achieved by using a localized dynamic model for the subgrid kinetic energy. Simultaneous to the solution of the gas phase equations, the liquid phase equations (5)-(11) are solved using the Lagrangian technique. The range of droplet sizes tracked in this scheme depends upon the computational constraints (which can be quite large if a large number of droplet sizes are to be tracked). The gas phase LES velocity field and the subgrid kinetic energy are used to estimate the instantaneous gas velocity at the droplet location. This essentially provides a coupling between the gas and liquid phase momentum transport. The gas phase scalar field evolution is simulated in the subgrid domain as discussed in the next section.

3. Subgrid Combustion Models

The principle difficulty in reacting LES simulations is the proper modeling of the combustion related terms involving the temperature and species, for example, the convective species fluxes such as $S_{\alpha j}$ due to subgrid fluctuations and the filtered species mass production rate $\overline{\dot{\omega}_\alpha}$. Probability density function methods when applied within LES either using assumed shape (Frankel et al., 1993) or evolution equation (Gao and O'Brien, 1993) may be used to close $\overline{\dot{\omega}_\alpha}$, and, in principle, any scalar correlations. However, the treatment of molecular mixing and small scale stirring using phenomenological models as in pdf methods have been only partially successful in predicting the mixing effects. Problems have also been noted when gradient diffusion assumption/eddy viscosity model is used to approximate the species transport terms. Use of this type of assumption for reactive species is dubious, as noted earlier (Dimotakis, 1989; Pope, 1979). Frankel et al. (1993) attributed the use of this assumption as the source of errors in the comparison of reacting LES simulations with DNS data.

Earlier, Kerstein (1989, 1992) developed a mixing model termed the linear eddy mixing (LEM) model and demonstrated its ability to separately treat the molecular diffusion and turbulent convective stirring processes at all relevant fluid mechanical length scales of the flow. The scalar fields are simulated within a 1D domain which represents a stochastic slice through the local scalar field. Within the context of LES, the LEM model is used to represent the effect of only the small unresolved scales on the scalar fields while the larger resolved turbulent scales of the flow are calculated directly from the LES equations of motion. To accomplish this, the mixing model is implemented within each LES cell. In the present investigation, the procedure for coupling the LEM model to the LES equations is essentially identical to the method developed earlier for gas-phase combustion (Menon at al., 1993a; Menon and Calhoon, 1996; Calhoon and Menon, 1996, 1997) and, therefore, is only summarized here.

The subgrid LEM has several advantages over conventional LES of reacting flows. In addition to providing a fundamentally accurate treatment of the small-scale turbulent mixing and molecular diffusion processes, this method avoids gradient diffusion modeling of scalar transport. Thus, both co- and counter-gradient diffusion can be simulated.

3.1 The Linear-Eddy Single Phase Model

The details of the baseline gas phase LEM model have been reported earlier (e.g., Kerstein, 1989, 1992; Menon et al., 1993a). Briefly, the exact reaction-diffusion equations (i.e., equation 4 without any LES filtering and without the convective term) are numerically solved using standard finite-difference scheme in the local 1-D domain using a grid fine enough to resolve the Kolmogorov and/or the Batchelor microscales. Consequently, the species production rate $\dot{\omega}_\alpha$ can be expressed in terms of the raw temperature and species fields without any modeling. This is a particularly attractive feature of the present model since it obviates the need for any modeling of the highly non-linear production terms.

Simultaneous to the deterministic evolution of the reaction-diffusion processes, turbulent convective stirring within the 1D domain is modeled by a stochastic mapping process (Kerstein 1992). This procedure models the mixing effect of turbulent eddies on the scalar fields and is implemented as an instantaneous rearrangement of the scalar fields without changing the magnitudes of the individual fluid elements, consistent with the concept of turbulent stirring. An underlying assumption employed here is that the subgrid turbulence is homogeneous and isotropic. Within the context of the LES, this is a reasonable assumption and is generally invoked for subgrid modeling.

The implementation of the stirring process requires (randomly) determining the eddy size l from a length scale pdf $f(l)$ in the range $\eta \le l \le l_{LEM}$ where, η is the Kolmogorov scale and l_{LEM} is the characteristic subgrid length scale which is currently assumed to be the local grid resolution Δ. A key feature of this approach is that this range of scales is determined from inertial range scaling as in 3D turbulence for a given subgrid Reynolds number: $Re_{LEM} = u' l_{LEM}/\nu$ where, u' is obtained from k^{sgs}. Thus, the range of eddy sizes and the stirring frequency (or event time) incorporates the fact that the small scales are 3D even though it is still implemented on the 1D stochastic domain. This feature is one of the major reasons for the past successes of LEM in gas phase diffusion flame studies (Menon and Calhoon, 1996; Calhoon and Menon, 1996, 1997). The details of the method to determine these parameters and the mapping procedure are given elsewhere (Kerstein 1992; Menon et al., 1993a) and, therefore, avoided here for brevity.

3.2 The Linear-Eddy Two-Phase Model

In the present formulation, the LEM reaction-diffusion equations have been modified to include the effects of droplets below a certain cut-off so that the final stages of droplet vaporization and mixing is included. As noted earlier, this approach overcomes the earlier limitations of the SSF where the droplets below certain size are assumed to instantaneously vaporize and mix. Implementation in the LEM requires a reevaluation of the basic LEM approach since droplet vaporization will change the subgrid mass of the gas (primarily the fuel). Thus, in addition to the scalar reaction-diffusion equations, mass equations needs to be included.

The presence of droplets have been incorporated into the LEM by assuming that the droplets act as a pseudo-fluid Thus, discrete droplets are not tracked as in the Lagrangian LES model but the overall effect of the small droplets within each LES cell is modeled in the LEM using a void (volume) fraction approach. This approach is valid only when the droplets form only a small fraction of the total volume. However, this is an acceptable assumption here since all droplets larger than the cutoff are still tracked using the Lagrangian approach. The present Eulerian two-phase approach is also preferred (in terms of accuracy) when compared to the Lagrangian approach when the droplets are very small and begin to behave more like a continuum fluid. The conservation of mass in both the phases in the LEM is given by the following relation:

$$\rho_g \varphi + \rho_l (1 - \varphi) = \rho_{avg} \tag{12}$$

where subscript g represents gas phase, l the liquid phase and φ is the volume fraction of the gas phase (1 - void fraction of the liquid (λ)). The void fraction λ or φ can be initially specified but evolves during the subgrid evolution. Although, the liquid density is a constant, the gas density ρ_g is not since there is mass addition from the liquid phase. Thus, ρ_g also needs to be determined. The equations governing the conservation of mass of the gas and liquid phases in the LEM are:

$$\frac{\partial \rho_g \varphi}{\partial t} = S_L + S_2 \tag{13}$$

$$\frac{\partial (1-\varphi)\rho_l}{\partial t} = S_1 - S_2 \tag{14}$$

Here, the source term S_1 is the contribution of the supergrid to the subgrid liquid phase when the droplet size falls below the cutoff. S_L is the term due to the vaporization of the droplets tracked in the supergrid, while S_2 represents the contribution from the subgrid vaporization of the liquid going into the gaseous phase. The droplets from the supergrid process contribute to the subgrid, if and only if the droplet size is smaller than the cutoff. If initially there are no drops below the cut-off size, then the formulation is identical to the pure gas-phase flow. Equations (13) and (14) are used to determine the gas density ρ_g and the volume fraction φ. An inherent assumption in equations (13) and (14) is that the source terms are obtained under the assumption that the droplets are so small that there is negligible relative motion between the liquid and gas phase. Although this assumption sounds reasonable (since droplets are very dilute and the liquid phase is behaving as a pseudo-fluid, this assumption still needs further justification and is an issue of current research).

The conversion of the subgrid droplets into gas phase is included as a source term in the gas phase species equation (only the fuel species is effected). Thus, the equation governing any scalar mass fraction (Ψ) in the subgrid can be written as

$$\frac{\partial \rho_g \varphi \psi}{\partial t} = D \frac{\partial^2 (\rho_g \varphi \psi)}{\partial s^2} + \dot{\omega}_\psi + S_\psi + S_L \qquad (15)$$

Here, "s" indicates that this equation is solved on the 1D domain of LEM. Also, $\dot{\omega}_\psi$ is the production/destruction of the species Ψ due to gas-phase chemical reactions and S_ψ is the source term for the production of the species due to vaporization of the liquid phase. Thus, S_ψ represents a source only in the fuel species equation. If S_ψ is neglected, the above equation is the same as in the earlier gas phase LEM approach. For heat release and droplet vaporization cases, a 1D temperature equation also needs to simulated in the subgrid as discussed in Calhoon and Menon (1997).

Another issue to be noted in equations (13)-(15) is that the convective term due to fluid motion is missing. This is consistent with the LEM approach, whereby, the convection of the scalar fields is modeled using the small-scale turbulent stirring and by the splicing process (described in section 3.3), as noted earlier (Kerstein, 1992; Menon et al., 1993a). An area for further investigation is the effect of stirring on the droplets. Currently, it is assumed that the droplets in the subgrid have no relative motion with respect to the gas phase. Thus, the rearrangement process used to model the effect of stirring on the gas species is also implemented unchanged to stir the droplets. If relative motion is to be included, some modifications to the stirring process may be required. This is an issue for future investigation.

3.3 Subgrid implementation of LEM

Since the filtered species $\overline{Y_\alpha}$ is calculated directly by filtering the subgrid Y_k fields, there is no need to solve the LES filtered equations (i.e., Eq. 4). Consequently, use of conventional (gradient diffusion) models is avoided. However, since the Y_k subgrid fields (in Eq. 15) are also influenced by large scale convection (due to the LES-resolved velocity field $\overline{u_i}$ and the subgrid turbulent fluctuation estimated from k^{sgs}), additional subgrid-supergrid coupling processes are required. Here, supergrid denotes the resolved scale field as computed by the LES equations.

The convection of the scalar fields by the supergrid field (supergrid-to-subgrid coupling) across LES cell faces is modeled by a "splicing" algorithm (Menon et al., 1993a; Menon and Calhoon, 1996; Calhoon and Menon, 1996). Details of this process is given in the cited references and, therefore, avoided here since the method for two-phase flows is identical to the one developed earlier for gas phase flows.

Thus, the subgrid and supergrid processes involve the following processes. Given the initial subgrid scalar fields and void fraction in each LES cell, droplet vaporization, molecular diffusion, chemical reaction, turbulent stirring, and large scale convection processes are implemented as discrete events occurring in time. The epochs of these processes are determined by their respective time scales. This type of discrete implementation is similar to the fractional step method used to solve differential equations.

As the subgrid scalar fields evolve under the action of these processes, the resolved LES fields (both the gas and liquid phases) are solved concurrently on the LES time scale(s). The resolved scales influence the evolution of the subgrid scalar fields via the specification of the subgrid length scale, the subgrid Re and the changes in the void fraction due to droplets vaporizing and becoming smaller that the cutoff size. The subgrid scalar fields in turn influence the development of the resolved scales (subgrid-to-supergrid coupling) by providing the filtered scalar fields, temperature-species correlations and the heat release calculated from the subgrid scalar fields.
The splicing algorithm employed in the present study

transports subgrid fluid elements from one LES cell to another based on the local velocity field. The local velocity consists of the resolved velocity $\overline{u_i}$ plus a fluctuating component (estimated from the subgrid kinetic energy). The splicing events are implemented discretely on the convective time scale (which is also the time-step for the gas phase LES). Each splicing event involves (1) the determination of volume transfer between adjacent LES grid cells, (2) the identification of the subgrid elements to be transferred, and (3) the actual transport of the identified fluid elements. The underlying rationale for this procedure has been discussed elsewhere (Menon et al., 1993a; Calhoon and Menon, 1996). The same splicing algorithm is used here except that now both the scalar fields and the void fraction in the subgrid field are spliced at the same time.

An important property of the splicing algorithm is that the species convection is treated as in Lagrangian schemes. Thus, convection is independent of the magnitude or gradient of the species which are transported and depends only on the velocity field. As a result, subgrid elements are transported without changing their species and temperature magnitudes. This property allows this algorithm to avoid difficulty of false numerical diffusion associated with the numerical approximation of convective terms in differential equations. By avoiding both numerical and gradient diffusion, the splicing algorithm allows an accurate picture of the small scale effects of molecular diffusion to be captured, including differential diffusion effects.

4. Results and Discussion

The two-phase LES model has been successfully implemented into a 3D zero-Mach number code developed earlier for gas phase combustion (Menon and Chakravarthy, 1996; Chakravarthy and Menon, 1997). Briefly, this code solves the gas phase LES equations on a non-staggered grid using a high-order finite difference scheme. Time integration is achieved using a two-step semi-implicit fractional step method that is second-order accurate. The spatial difference scheme is fifth-order for the convective terms and fourth-order for the viscous term. The Poisson equation for pressure is solved numerically using a second-order accurate elliptic solver that uses a four-level multigrid scheme to converge the solutions.

The Lagrangian tracking of the droplets in the LES domain is carried out using a fourth-order Runge-Kutta scheme. The number of droplets tracked in the LES is determined at present by the computational constraints. However, more detailed studies are planned in the future to determine an optimum cut-off size.

In the following, some preliminary results are discussed focussing primarily on the subgrid model since the Lagrangian LES approach is conventional (e.g. Oefelein and Yang, 1996) and well established. First, using an exact solution of a decaying vortex, the trajectories of the injected droplets is simulated. Then, simulations were carried out in a 3D temporal mixing layer with droplet continuously injected in the core of the mixing layer. Subsequently, the initial droplet void fraction in each LES cell is determined based on a specified droplet cut-off size. Using this initial conditions, droplet vaporization, turbulent mixing and infinite rate chemical reactions (with no heat release) are studied within the subgrid. No coupling between the supergrid and subgrid is included here. Coupling (via the splicing technique) is currently available and can be included without any modifications to the code. Fully coupled LES-LEM will be discussed at a later date (Pannala and Menon, 1998).

Infinite rate kinetics in the subgrid is studied without any direct influence from the Lagrangian LES part (other than providing the initial conditions). Thus, the source term S_1 in equation (14) is reflected as the initial void fraction of the fuel and term S_L in equation (13) and (15) goes to zero. The source term for the subgrid vaporization is given as: $S_2 = n_p \dot{m}_p$, where n_p is the number of droplets (determined initially from the droplet cut-off size and the initial volume fraction $(1-\varphi)$ of the droplets in the subgrid). Once n_p is determined for each LES cell, it is assumed to be constant. However, the droplet size is still allowed to decrease due to vaporization. This assumption will be relaxed in the future especially when the large-scale convection via splicing is included.

The mass transfer rate $\dot{m}_p$ is determined from the relation: $\dot{m}_p = 2\pi\rho_g D_g d_p \ln(1+B_M)$, which is similar to the mass rate used in the Lagrangian LES for the quiescent case (i.e., for no relative motion between gas and droplets). Here, the subscript "g" indicates the gas property at the droplet surface and the droplet diameter is determined from the void fraction by the relation:

$$d_p = 2\delta\left(\frac{1-\varphi}{n_p\frac{4\pi}{3}}\right)^{1/3} \tag{16}$$

Here, δ is the subgrid resolution (determined based on the requirement that the Kolmogorov eddy must be resolved). Finally, the scalar equation (15) is replaced for infinite rate kinetics by equations for the fuel and

oxidizer mass fractions. The source term S_ψ is non-zero only for the fuel species equation and is given as: $S_\psi = n_p \dot{m}_p$. Also, for present, equal diffusivity for the fuel and oxidizer is assumed.

Using the exact solution of a decaying vortex, the dispersion of the droplets is first investigated. Five different sized particles are injected in the core of the vortex in the x-direction with a specified velocity. The subsequent trajectories of these particles is tracked. Figure 1a shows the velocity vector field and Fig. 1b shows the trajectories of the injected droplets. It can be seen that the smaller particles follow the vortex streamlines while the larger particles follow independent paths due to their inertia. This qualitatively confirms that the Lagrangian particle tracking model in the LES code is implemented correctly. To obtain quantitative verification, an experimental study is underway at Georgia Tech to obtain data for code validation (currently no such data exists).

To evaluate the LES and subgrid two-phase LEM model, a 3D temporal mixing layer is simulated using a well established procedure. The mixing layer (slip walls in the transverse and periodic in streamwise and spanwise directions) is initialized using a tangent hyperbolic mean velocity along with the most unstable 2D mode and a 3D mode (this initialization is similar to that described in McMurtry et al., 1989). A grid resolution of 49x49x33 is used for the LES. As noted earlier, the goal here is primarily to investigate the subgrid model given initial states in the LES cells. To accomplish this, the 3D mixing layer is initialized by injecting droplets randomly in the mid spanwise plane with velocity magnitude randomly varying in the range 0-30 m/s. The droplets in three groups: 60, 20 and 7.5 μm are injected continuously in this mid spanwise plane. As the mixing layer evolves in time and coherent 2D spanwise structures evolve, the droplet distribution is tracked using the Lagrangian method.

Figures 2a and 2b show, respectively, two typical stages of evolution of the mixing layer in terms of the vorticity contours. The corresponding droplet distribution at this stage are shown in Figs 3a and 3b, respectively. As can be seen, the smaller particles are entrained into the core of the vortex while the larger particles are not.

The contribution of the Lagrangian droplets to the subgrid void fractions in the LES cells is then determined by assuming a cut-off size of 10 microns. Figure 4 shows the computed void fraction in the LES cells along the streamwise direction at the center mid plane. Since most of the smaller droplets are concentrated in the core, the volume fraction of the fuel is much higher there than at other locations. These values of void fraction then become the initial conditions for the subgrid evolution in each LES cell. Figure 5 shows the typical distribution of the void fraction over the entire domain. For the LES case studied here only a small fraction of the domain contains droplets smaller that the Lagrangian cut-off size. However, note that in an actual reacting LES there is likely to be more cells containing non-zero void fraction. In any event, due to unequal distribution of the void fraction of the fuel in the subgrid, the subgrid LEM is not required at every LES grid point. This implies that proper dynamic load balancing needs to be incorporated when attempting parallel simulations of this LES approach.

The initial subgrid void fractions are very small. However, note that since the liquid density is very large, the overall mass of the liquid droplets is quite significant. Since we are not simulating the coupled LES-LEM model, only the initial states from the LES is used for the LEM simulations. Also, the subgrid processes evolve independently between consecutive LES time steps. Here, the evolution of the subgrid Eulerian field as a function of some relevant parameters is investigated. These parameters are: the initial subgrid temperature, the initial volume fraction and the subgrid turbulence. Some characteristic results are summarized below.

Since there is no data to validate the subgrid vaporization model discussed here, we first compare the current predictions with results obtained earlier by McMurtry et al. (1993) who employed the LEM in a stand-alone mode to study decay of a non-reactive scalar field. Here, using very similar initialization, the decay of a scalar was investigated in the presence of droplet vaporization. A range of initial values of the void fraction was used for these simulations. As shown in Fig. 6, as the droplet evaporates and the void fraction tends to zero (or $\varphi \rightarrow 1$), the scalar variance approaches the value predicted by McMurtry et al. (1993) in the absence of droplets.

In Fig. 7, the product mass fraction evolution in time (subgrid time between two LES time steps) is shown for a range of initial values of void fraction under otherwise identical conditions. The product formation increases in time and with increase in the initial void fraction of fuel. However, since the vaporization process is endothermic and non-linear (initially very high but levels off in time as temperature fall), the product increase is also non-linear (product formation and vaporization have a direct correspondence). Figure 8 shows the product mass fraction increases with initial liquid and gas temperature. At present, it is assumed that both gas and liquid is at the

same temperature (or that there is infinite conductivity in the subgrid). However, this assumption can be relaxed. An increase of 100 K in the temperature increases the initial vaporization rate considerably and this results in much larger amount of product formed.

Finally, Fig. 9 shows the effect of changing the subgrid Re (or the turbulent mixing rate) on the product formation. A physical reasoning for the observed decrease in product formation with increase in subgrid Re is not available at present. Decrease in product formation is directly due to a decrease in the vaporization rate. In the current vaporization model, the estimate for the Spalding number B_M plays a direct role in the estimate of the vaporization rate. This parameter depends on the process of diffusion of fuel from the droplet surface to the surrounding gas. Current equal diffusivity approach needs to be reevaluated to address this effect. Also, there is likely to be some subtle effect of the rearrangement process used to model the mixing process. Increase in the subgrid Re changes both the typical eddy size and the event frequency used to carry out small scale mixing. How this impacts the vaporization process is an issue under study.

5. Conclusions

In this study, a gas phase subgrid combustion model developed earlier has been extended for application in two-phase flows. This approach includes a more fundamental treatment of the effects of the final stages of droplet vaporization, molecular diffusion, chemical reactions and small scale turbulent stirring than other LES closure techniques. As a result, Reynolds, Schmidt and Damkohler number effects are explicitly included. This model has been implemented within an Eulerian-Lagrangian two phase large-eddy simulation (LES) formulation. In this approach, the liquid droplets are tracked using the Lagrangian approach up to a prespecified cut-off size. The evaporation and mixing of the droplets smaller than the cutoff size is modeled within the subgrid using an Eulerian two-phase model that is an extension of the earlier gas-phase subgrid model. The issues (both resolved and unresolved) related to the implementation of this subgrid model within the LES are discussed in this paper along with some preliminary results that demonstrate its capabilities.

Acknowledgments

This work was supported in part by the Army Research Office Multidisciplinary University Research Initiative grant DAAH04-96-1-0008 and by the Air Force Office of Scientific Research Focussed Research Initiative contract F49620-95-C-0080 monitored by General Electric Aircraft Engine Company, Cincinnati, Ohio.

References:

Calhoon, W.H. and Menon, S. (1996) "Subgrid Modeling for Reacting Large-Eddy Simulations," AIAA 96-0516, 34th AIAA Aerospace Sciences Meeting, Reno, NV, Jan. 15-18.

Calhoon, W.H. and Menon, S. (1997) "Linear-Eddy Subgrid Model for Reacting Large-Eddy Simulations: Heat Release Effects," AIAA 97-0368, 35th AIAA Aerospace Sciences Meeting, Reno, NV, Jan. 6-10.

Chakravarthy, V. K. and Menon, S. (1997) "Characteristics of a Subgrid Model for Turbulent Premixed Combustion," AIAA Paper No. 97-3331, 33rd AIAA/ASME/SAE/ASEE Joint Propulsion Conference and Exhibit, Seattle, Wa, July 6-9.

Chen, K-H., Duncan, B., Fricker, D., Lee, J., and Quealy, A. (1996) "ALLSPD-3D USER MANUAL," Internal Fluid Mechanics Division, NASA Lewis Research Center.

Chen, K-H. and Shuen, J.-S. (1993) "A Coupled Multi-Block Solution Procedure for Spray Combustion in Complex Geometries," AIAA 93-0108, 31st AIAA Aerospace Sciences Meeting, Reno, NV.

Dimotakis, P. E. (1989) "Turbulent Free Shear Layer Mixing," AIAA Paper 89-0262, 27th Aerospace Sciences Meeting, Reno, Nevada.

Faeth, G. M. (1983) "Evaporation and Combustion of Sprays," Progress in Energy and Combustion Science, Vol. 9, pp. 1-76.

Frankel, S. H., Adumitroaie, V., Madnia, C. K., and Givi, P. (1993) "Large Eddy Simulation of Turbulent Reacting Flows by Assumed pdf Methods," in Engineering Application of Large Eddy Simulations, Ragab, S. A., and Piomelli, U., ed., ASME, FED-Vol. 162, New York, pp. 81-101.

Gao, F., and O'Brien, E. E. (1993) "A Large-Eddy Simulation Scheme for Turbulent Reacting Flows," Physics of Fluids A, Vol. 5, pp. 1282--1284.

Kerstein, A. R. (1989) "Linear-Eddy Model of Turbulent Transport II. Application to Shear Layer Mixing, Combustion and Flame," Vol. 75, pp. 397--413.

Kerstein, A. R. (1992) "Linear-Eddy Model of Turbulent Transport 4. Structure of Diffusion-Flames," Comb. Sci. and Tech., Vol. 81, pp.75--96.

Kim, W. -W. and Menon, S. (1995) "A New Dynamic One-Equation Subgrid Scale Model for Large Eddy Simulation," AIAA 95-0356, 33rd Aerospace Sciences Meeting, Reno, NV, Jan. 9-12.

McMurtry, P. A., Riley, J. J., and Metcalfe, R. W. (1989) "Effects of Heat Release on the Large-scale Structure in Turbulent Mixing Layers," Journal of Fluid Mech., Vol. 199, pp. 297-332.

McMurtry, P., Gansauge, T., Kerstein, A. R., and Krueger, S. K. (1993) "Linear Eddy Simulations of Mixing in a Homogeneous Turbulent Flow," Phys. of Fluids, Vol. 5, No. 4, pp. 1023-1034.

Menon, S., McMurtry, P., and Kerstein, A.R. (1993a) "A Linear Eddy Mixing Model for LES of Turbulent Combustion," in Large-Eddy Simulations of Complex Engineering and Geophysical Flows, (B. Galperin and S.A. Orszag, Eds.), Cambridge University Press, pp. 278-315.

Menon, S., McMurtry, P., and Kerstein, A.R. (1993b) "A Linear-Eddy Subgrid for Turbulent Combustion: Application to Premixed Combustion," AIAA Paper No. 93-0107, 31st Aerospace Sciences Meeting, Reno, NV, Jan. 11-14.

Menon, S. and Chakravarthy, V. K. (1996) "Large-Eddy Simulations of Premixed Flames in Couette Flow," AIAA 96-3077, 32nd AIAA/ASME/SAE/ASEE Joint Propulsion Conference, Lake Buena Vista, FL, July 1-.3,

Menon, S. and Kim, W.-W. (1996) "High Reynolds number flow simulations using the localized dynamic subgrid-scale model," AIAA 96-0425, 34th AIAA Aerospace Sciences Meeting, Reno, NV, Jan. 15-18.

Menon, S. and Calhoon, W. (1996) "Subgrid Mixing and Molecular Transport Modeling for Large-Eddy Simulations of Turbulent Reacting Flows," Symp. (International) on Combustion, 26.

Mostafa, A. A. and Mongia, H. C. (1983) "On the Modeling of Turbulent Evaporating Sprays: Eulerian versus Lagrangian Approach," Int. J. of Heat Mass Transfer, Vol. 30, pp. 2583-2593.

Oefelein, J. C. and Yang, Y. (1996) "Analysis of Transcritical Spray Phenomena in Turbulent Mixing Layers," AIAA 96-0085, 34th AIAA Aerospace Sciences Meeting, Reno, NV, Jan. 15-18.

Pannala, S. and Menon, S. (1998) "Large-Eddy Simulations of Two-Phase Turbulent Flows," to be presented at 36th AIAA Aerospace Sciences Meeting, Reno, NV, Jan. 12-15.

Pope, S. B. (1979) "The Statistical Theory of Turbulent Flames," Philosophical Trans. of the Royal Soc. of London, Vol. 291, pp. 529--568.

Poinsot, T. (1996) "Using Direct Numerical Simulations to Understand Premixed Turbulent Combustion," Symp. (Intn.) on Combustion, 26, pp. 219-232.

Smith. T. M. and Menon. S. (1997) "Large-Eddy Simulations of Turbulent Reacting Stagnation Point Flows," 35th AIAA Aerospace Sciences Meeting, Reno, NV, Jan. 6-10.

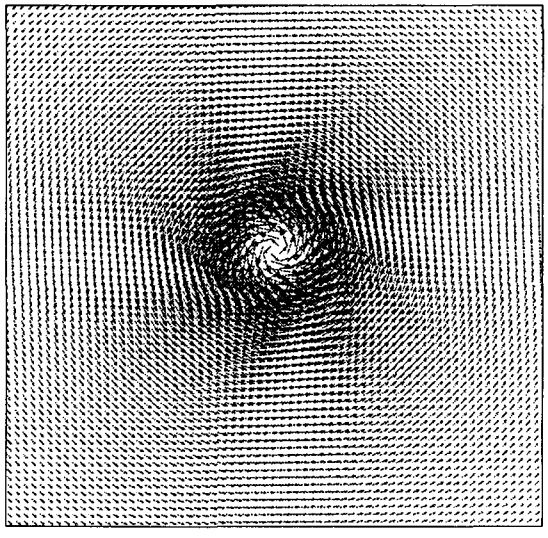

Figure 1 a) The velocity vector field around the core of a decaying vortex.

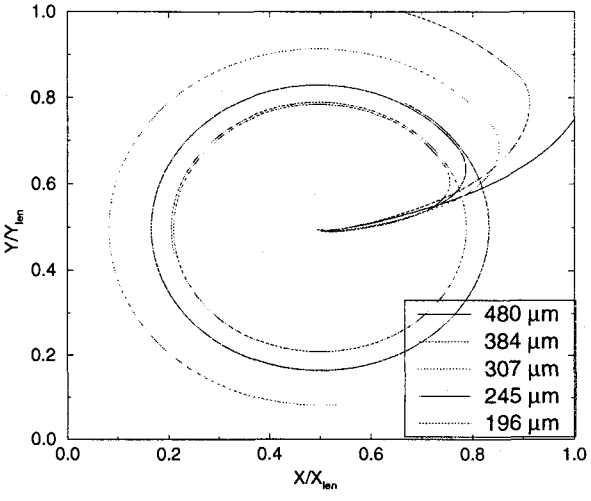

Figure 1 b) Trajectories of the particles injected into above decaying vortex. Smaller particles following the vortex while the bigger particles tend to retain their initial path.

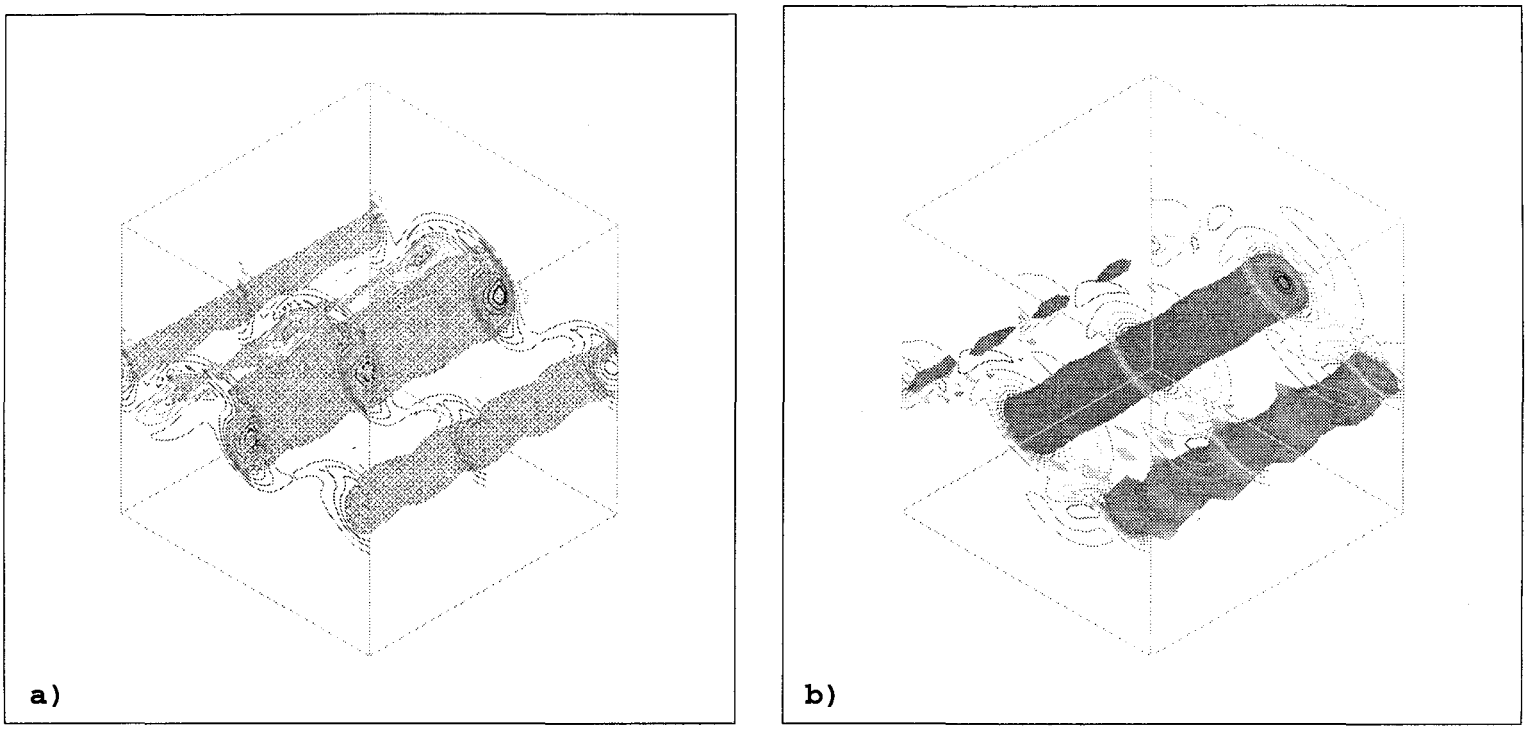

Figure 2. 3D perspective of mixing layer. Iso-surface corresponding of abs(ω) = 0.707. Also shown are the z-vortcity contours at three planes. a) τ = 5 & b) τ = 15. Here t is normalized time by the initial $[\delta \bar{u}/\delta y]^{-1}$

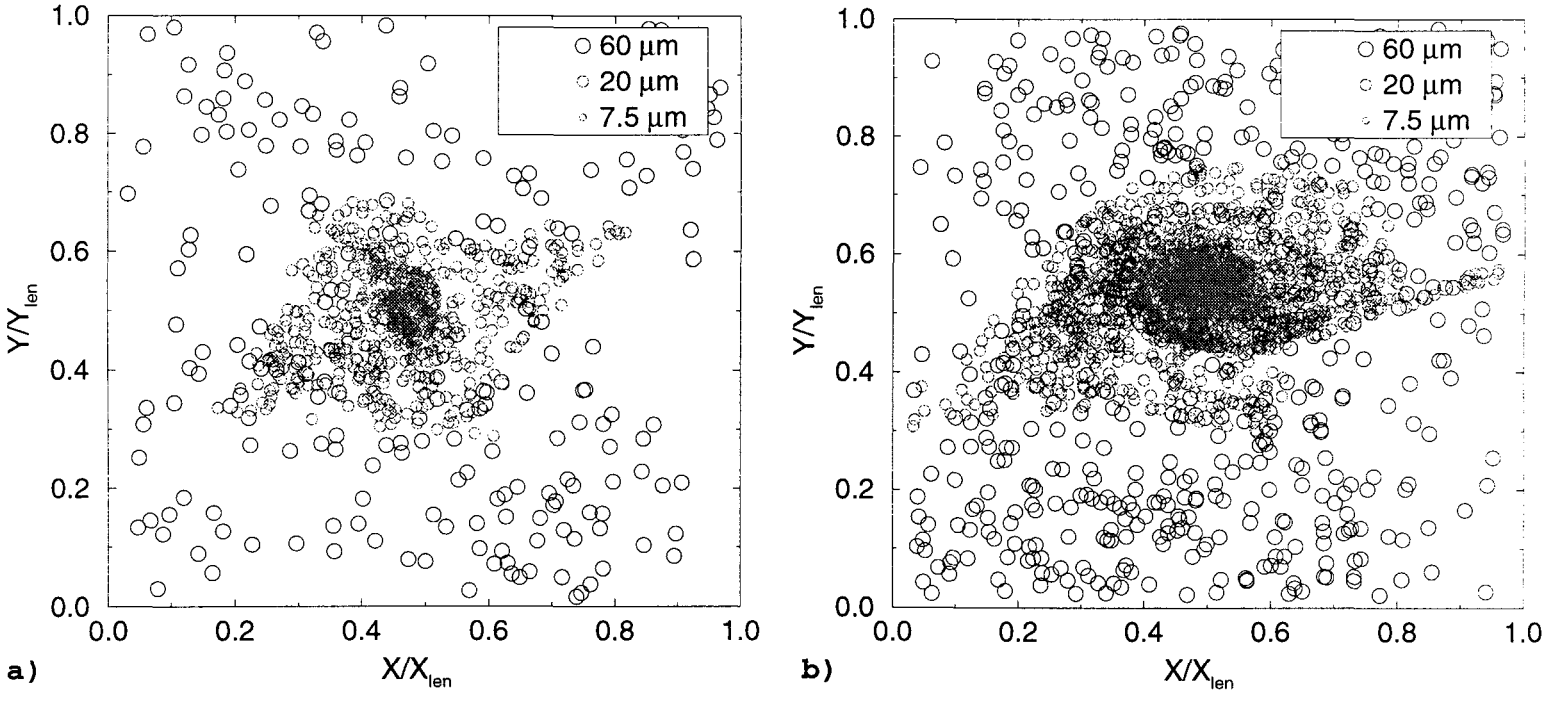

Figure 3. Spatial distribution in the (X-Y) plane of particles injected into the center (mid span plane) of the mixing layer. As can be seen the smaller particles are entrained into the vortex core when compared to the larger particles. a) τ = 5 & b) τ = 15. The X,Y distances are normalized by respective domain lengths.

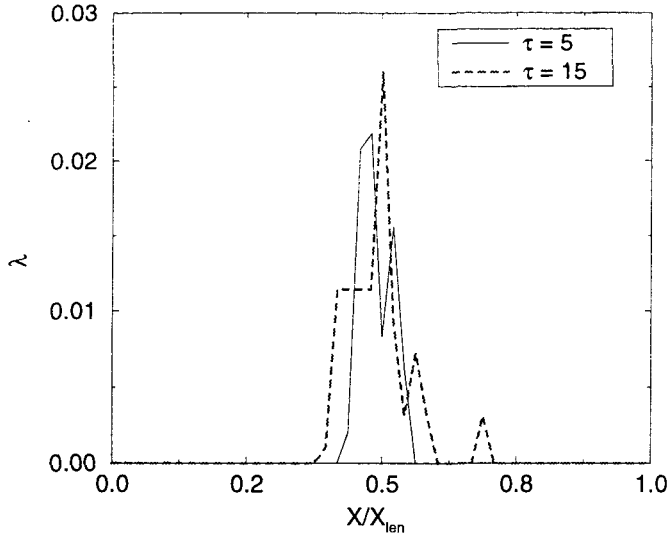

Figure 4. Supergrid contribution to the subgrid liquid volume fraction λ along a line through the vortex core.

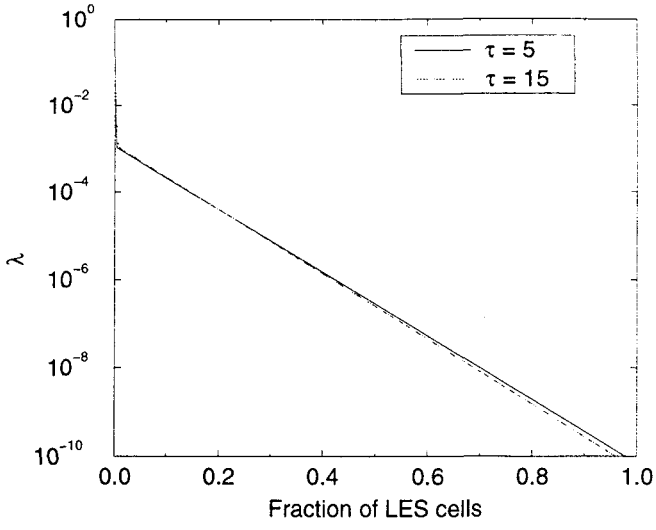

Figure 5. Distribution of subgrid liquid volume fraction in the 3D mixing layer.

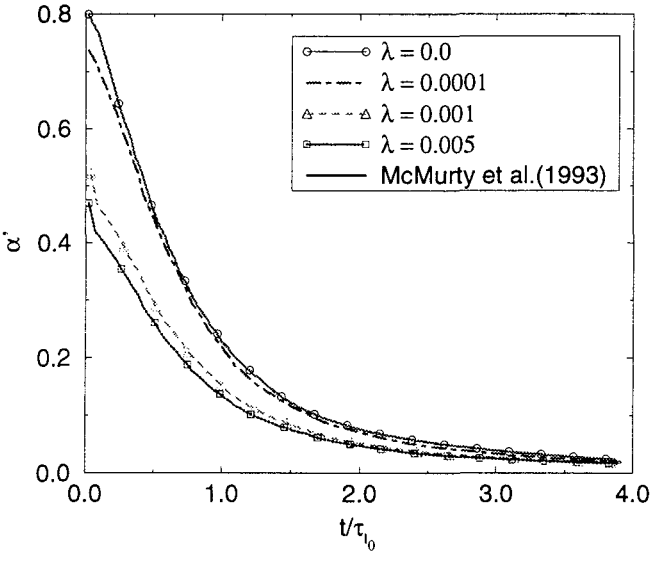

Figure 6. Time evolution of a passive scalar rms for different initial void fractions for Re_{sgs} = 90 and T = 400 K.

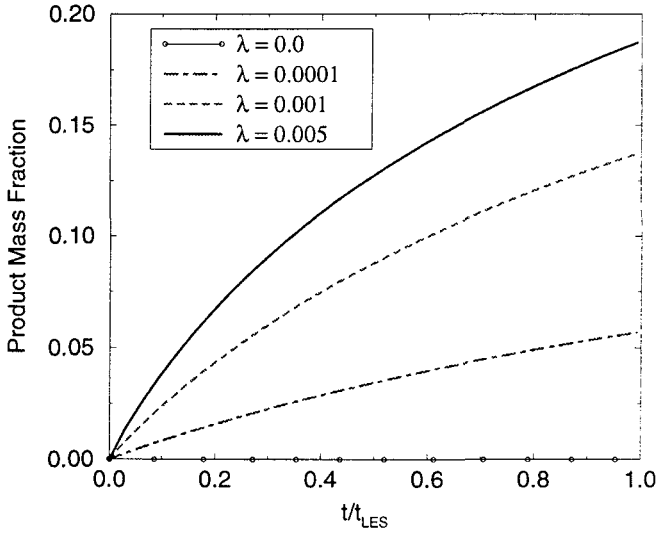

Figure 7. Time evolution of product mass fraction for different fuel volume fractions at Re_{sgs} = 90 and T = 350 K

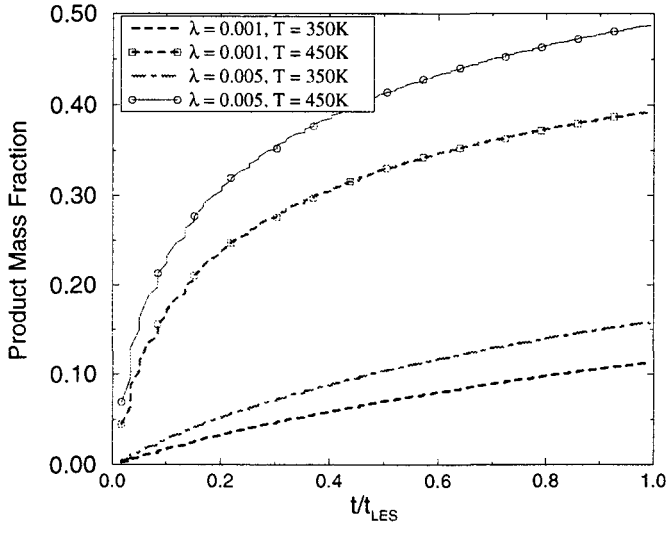

Figure 8. Variation of product mass fraction in a LES time step with temperature and λ at Re_{sgs} = 90.0

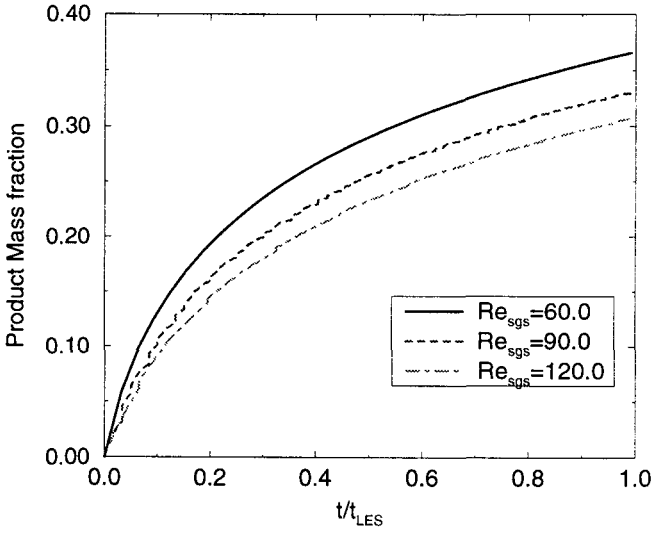

Figure 9. Variation of product mass fraction in a LES time step with Re_{sgs} at λ = 0.005 and T = 400 K